Water and Salt Transport Properties of Pentiptycene-Containing Sulfonated Polysulfones for Desalination Membrane Applications

Tao Wang, Feng Gao, Si Li, William A. Phillip, Ruilan Guo*

Department of Chemical and Biomolecular Engineering, University of Notre Dame, Notre Dame, IN, USA

***Correspondence:**
Professor Ruilan Guo
rguo@nd.edu

Highlights:

- Pentiptycene structure units were incorporated into sulfonated polysulfones.
- Defect-free thin films were solution casted for reverse osmosis tests.
- Water permeability and water/salt selectivity were simultaneously improved.
- Enhanced diffusivity selectivity led to the improved permeability-selectivity.
- High rejection performance was achieved with decent water permeability.

Graphical abstract:

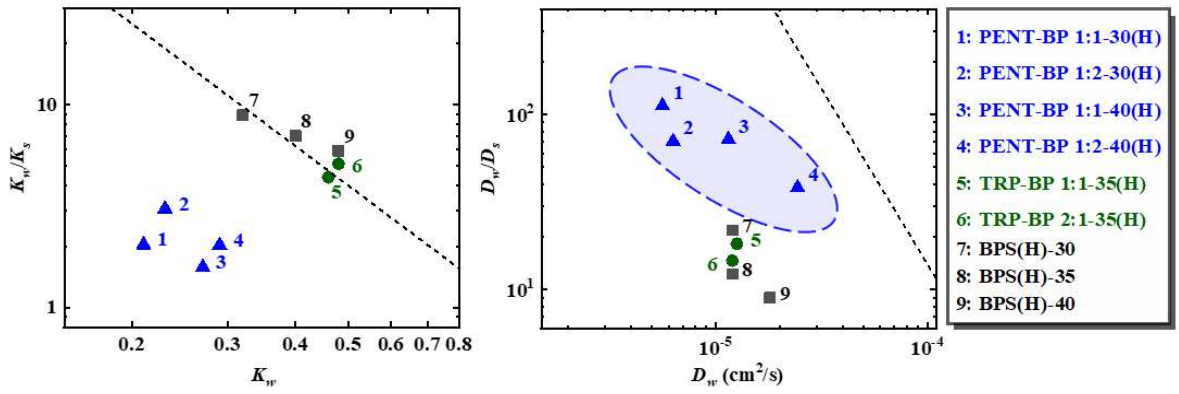

Abstract:

A series of pentiptycene-containing disulfonated polysulfone copolymers (PENT-BP) were synthesized via condensation polymerization. Water and salt transport properties (solubility, diffusivity and permeability) were characterized for acid-form membranes (PENT-BP(H)) and compared with triptycene-based sulfonated polysulfones (TRP-BP(H)) and a non-iptycene-containing 4,4'-biphenol-based series (BPS(H)) of polysulfones to investigate the effect of pentiptycene on membrane performance. At comparable water content, the PENT-BP(H) exhibited increased water and salt permeability due to the additional free volume introduced by the pentiptycene units. Enhanced water/salt permeability selectivity of PENT-BP(H) series was also observed due to a significantly higher diffusivity selectivity. At comparable water permeance ($P_w^D \sim 8 \times 10^{-6}\ cm^2/s$), the salt rejection of PENT-BP (H) copolymers obtained from dead-end filtration reached 91-93% at 400 psi, higher than that of a corresponding BPS(H) series. This study suggests that incorporation of iptycene moieties into polymer backbone is an effective strategy to enhance desalination membrane performance.

Keywords: reverse osmosis, pentiptycene, sulfonated polysulfone, water/salt selectivity, solution-diffusion model

1. Introduction

With 97% of the earth's water found in ocean, less than 1% of the earth's water is available freshwater [1]. Upon the global population expansion and industrialization, the demand for fresh water has become a serious issue [2–4]. Today, membrane-based technology, in particular, reverse osmosis (RO), is the most widely used technology for desalination applications due to their cost effectiveness and high energy efficiency [1,5–7]. The state-of-the-art RO membranes are polyamide-based membranes [8–10], which dominate the desalination market for high salt rejection and stable performance over wide ranges of feeding pH, temperature and pressure [5]. However, the amide linkages have poor tolerance to oxidizing agents such as chlorine-based disinfectants [11–13], which are widely used in water purifications to control biofouling. For this reason, the feeding water must be dechlorinated before reaching the polyamide membranes to avoid oxidative degradation and then rechlorinated after desalination process to prevent biofouling [14], which significantly increases the desalination costs.

Recently, poly(arylene ether sulfone)s have been studied in water treatments for their economic propensity, excellent thermal and mechanical stabilities as well as their chlorine tolerance [14,15]. To compensate the hydrophobicity of polymer backbones, sulfonation strategy has been widely used to increase the membrane hydrophilicity for enhanced desalination performance. Compared to post-polymerization sulfonation, direct copolymerization of disulfonated monomer, i.e., 3,3′-disulfonated-4,4′-dichlorodiphenyl sulfone (SDCDPS), into polysulfones has proved to be highly controllable and reproducible to achieve desired sulfonation degree and control the distribution of ionic groups [14–17]. While previous studies reported that BPS(H) polysulfones prepared from 4,4'-biphenol are promising for desalination applications due to their excellent chlorine tolerance [14], further fundamental studies of water and salt

transport properties of BPS(H) copolymers revealed that the polymer design of sulfonated polysulfones can be further optimized to simultaneously achieve high water permeability and water salt sieving ability (i.e., selectivity) [16].

In our recently reported study, a bulky building block of triptycene-containing structure was introduced into sulfonated polysulfone backbone (i.e., TRP-BP series) attempting to enhance the desalination performance[18]. It showed that the hierarchical triptycene units could effectively disrupt the chain packing and regulate the free volume distribution, suppressing both water and salt diffusion coefficients. The observed enhancement of water/salt selectivity of triptycene-containing sulfonated polysulfones, especially in the acid-form (i.e., TRP-BP(H) series), suggested that incorporating bulky and hierarchical structural units into sulfonated polysulfone backbones holds good promise for enhanced desalination performance. In this regard, we are motivated to extend the design of sulfonated polysulfone to include an even bulkier and more hierarchical iptycene unit – pentiptycene. Pentiptycene, an extension of triptycene composing five fused arene rings, has demonstrated great potential as high-performance gas separation membranes [19–24]. The well-defined molecular microcavities of pentiptycene scaffold provide an effective tool to selectively sieve gas molecules [19,25–27]. Given the similar transport mechanism in gas separation and desalination process [28,29], incorporating pentiptycene into sulfonated polysulfones might further enhance the desalination performance.

Hereby, a series of pentiptycene-containing sulfonated polysulfones (PENT-BP) with systematically varied sulfonation degree and pentiptycene content were synthesized and the fundamental water and salt transport properties of acid-form membranes were characterized. Direct comparisons between pentiptycene-based PENT-BP series, triptycene-based TRP-BP series and non-iptycene containing BPS series were made to elucidate the pentiptycene effect on

water and salt transport properties. Water and salt solubility, diffusivity, permeability and salt rejection were reported for all three series of sulfonated polysulfones, wherein PENT-BP(H) series exhibited simultaneously improved water permeance and water/salt selectivity as well as higher salt rejection.

2. Experimental

2.1. Materials

Pentiptycene-6,13-diol (PENT) was synthesized according to previous literature[30][31]. Anthracene, sodium hydrosulfite and 4,4'-difluorodiphenylsulfone (DFDPS) were purchased from Alfa Aesar and used as received.1,4-benzoquinone, tetrachloro-1,4-benzoquinone, potassium carbonate, sodium chloride, sodium bicarbonate, acetic acid, dimethyl sulfoxide-d_6 and methanol were purchased from Sigma-Aldrich and used as received. 4,4'-biphenol (BP) and 3,3'-disulfonated-4,4'-dichlorodiphenylsulfone (SDCDPS) were purchased from Akron Polymer Systems and dried in vacuum at 110 °C for 24 h before use. Anhydrous N, N-dimethylacetamide (DMAc) and toluene were purchased from EMD Millipore and used as received. Deionized water (DI water) was obtained from a Millipore water purification system (Milli-Q Advantage A10, Milli-Q, Billerica, MA).

2.2. Polymer synthesis and film preparation

Pentiptycene-containing disulfonated copolymers with controlled pentiptycene molar content and sulfonation degree were synthesized via polycondensation of PENT, BP, DFDPS and SDCDPS in predetermined ratios through nucleophilic aromatic substitution mechanism (S_NAr) according to our previously reported procedures with some modifications (Scheme 1) [18]. The nomenclature used for the copolymers is PENT-BP a:b-S, where a:b is the PENT:BP molar ratio and S is the molar percentage of sulfonated SDCDPS in the copolymers, as shown in Scheme 1.

It should be noted that copolymers with high PENT molar content (> 50 mol%) and high degree of sulfonation (>50%) didn't have sufficiently high molecular weight for film formation due to the low reactivity between PENT and SDCDPS and the poor solubility of the corresponding copolymers. Detailed synthesis procedures are described as follows using PENT-BP 1:2-40 as an example: 2.3127 g PENT (5 mmol), 1.8621 g BP (10 mmol), 2.9772 g SDCDPS (6 mmol), 2.3113 g DFDPS (9 mmol) and 4.1879 g K_2CO_3 (30 mmol) were charged into a 100 mL three-neck flask equipped with a nitrogen inlet, a mechanical stirrer and a Dean-Stark trap. Then 50 mL anhydrous DMAc and 25 mL toluene were added and the reaction mixture was refluxed at 145 °C for 4 h to dehydrate the system. While removing the toluene, the temperature was slowly increased to 185 °C and held for 72 h with stirring and nitrogen purge. The resulting viscous polymer solution was filtered to remove salts and then precipitated in stirring methanol. The fibrous copolymer was then collected and dried in vacuum oven for 24 h at 120 °C.

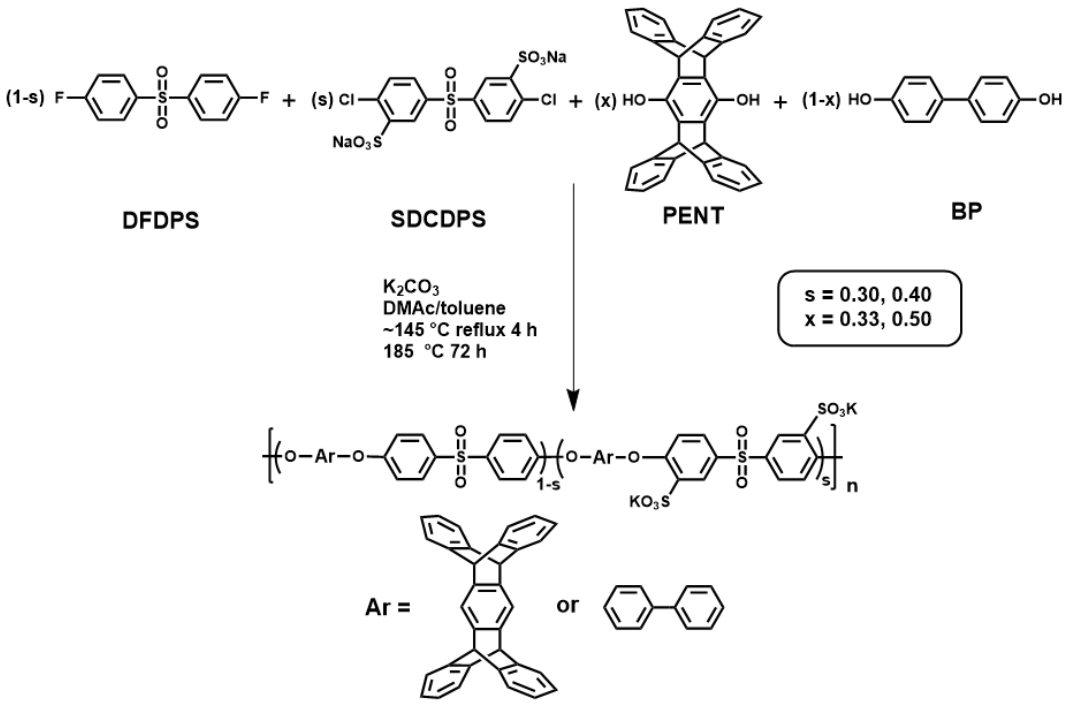

Scheme 1. Synthesis of PENT-BP random copolymers with controlled composition and degree of sulfonation.

To prepare salt-form thin films, the as-prepared copolymers were dissolved in DMAc to form ~7% w/v solutions, which were then filtered through 0.45 μm Teflon® syringe filters. The filtered solutions were cast onto clean, leveled glass plates and dried under an infrared lamp at ~55 °C for 24 h to form polymer films. The residual solvent was removed by drying the films under vacuum at 120 °C for 24 h.

To prepare acid-form films, where K^+ is replaced with H^+ in the PENT-BP structure shown in Scheme 1, the as-cast salt-form thin films were boiled in 0.5 M sulfuric acid solution for 2 h followed by hot deionized (DI) water boiling for another 2 h following a previously reported method [32]. For the acid-form polysulfone films, "(H)" is added as a suffix to the names of corresponding salt-form copolymers to indicate they are in acid form. For example, PENT-BP 1:2-40(H) is the acidified form of PENT-BP 1:2-40 that has 33 mol% pentiptycene and 40% sulfonation degree. All obtained thin films with thickness between 40~70 μm were stored in DI water before measurements.

2.3. Polymer and film characterization

The chemical structures and the composition of pentiptycene-containing disulfonated copolymers were confirmed by ^{1}H NMR spectroscopy on Bruker AVANCE III HD 400 Nanobay spectrometer with tetramethylsilane (TMS) as the internal standard. The dry-weight ion exchange capacity (IEC, meq/g) of all acid-form membranes was determined by acid-base titration method following previously reported procedure [17]. The details of mechanical property measurement and results were reported in supplementary information.

140 The density of dry acid-form films was measured using a density measurement kit (ML-DNY-43,
141 Mettler Toledo) and an analytical balance (ML204, Metter Toledo) at room temperature using
142 cyclohexane as a medium. The dry film density, ρ_{dry}, was determined according to Archimedes'
143 principle (Eq. 1):

144 $$\rho_{dry} = \frac{m_{air}}{m_{air} - m_{wet}} (\rho_{aux} - \rho_{air}) \quad (1)$$

145 where m_{air} is the dry film weight measured in air and m_{wet} is measured in cyclohexane. The
146 density of cyclohexane, ρ_{aux}, was determined at room temperature and ρ_{air} was taken as 0.0012
147 g/cm^3 [18].

148 *2.4. Water transport measurements*

149 The water uptake (WU) of acid-form membranes was evaluated by immersing fully dried
150 polymer films in DI water at room temperature and weighed periodically until a stable reading
151 was obtained (m_{wet}). Specifically, the hydrated membrane was wiped using Kimwipe® to remove
152 surface water and quickly weighed. The dried membrane (m_{dry}) was weighed using an analytical
153 balance immediately after being dried in vacuum oven at 100 °C for 24 h. WU was then
154 calculated from Eq. 2,

155 $$WU = \frac{m_{wet} - m_{dry}}{m_{dry}} \quad (2)$$

156 The equilibrium volume fraction of water in the hydrated membrane, ϕ_w, was calculated by
157 assuming ideal mixing behavior between water and polymer [16]:

158 $$\phi_w = \frac{WU/\rho_w}{WU/\rho_w + 1/\rho_{dry}} \quad (3)$$

The water partition coefficient, or, water sorption coefficient, K_w, is defined as the ratio of water concentration in the film, C_w^m (grams of water per cubic centimeter of hydrated film), to external water concentration, C_w (grams of water per cubic centimeter of external solution):

$$K_w = \frac{C_w^m}{C_w} \tag{4}$$

where C_w is equal to the density of pure water, taken as 1 g/cm^3 at room temperature [28]. K_w is related to the volume fraction of water, ϕ_w (Eq. 3), as follows:

$$K_w = \frac{\phi_w M_w}{C_w \bar{V}_w} \tag{5}$$

where M_w is the molecular weight of water, 18 g/mol and $\bar{V}_w$ is the molar volume of water at room temperature, taken as 18 cm^3/mol. By combining Eq. 4 and Eq. 5, the water partition coefficient K_w was equal to the equilibrium volume fraction of water in a hydrated membrane:

$$K_w = \phi_w \tag{6}$$

Water flux, J_w, was measured using dead-end filtration with an Amicon 8003 stirred cell (Millipore). Hydrated PENT-BP membranes were cut into 1-inch diameter discs and mounted in the base of the cell, which was then filled with DI water. The cell was connected to a source of compressed nitrogen, which drove the flow of DI water at applied pressures of 50, 60,70 psi (3.45, 4.14, 4.83 bar) separately. At each pressure, permeate weight was collected in a 20 mL scintillation vial on an analytical balance (Denver Instrument PI-4002) as a function of time and then converted to volume to determine the permeation rate. The vial was sealed with Parafilm to minimize evaporation. The water flux (J_w) was calculated from the volumetric permeation rate ($\Delta V/\Delta t$) as follows,

$$J_w = \frac{\Delta V}{A_w \cdot \Delta t} \quad (7)$$

where A_w is the effective area of a membrane disc within the stirred cell. Hydraulic water permeability, P_w^H, was then calculated as[28]

$$P_w^H = \frac{J_w l}{\Delta p} \quad (8)$$

where l is the thickness of hydrated membrane measured immediately after the flux test and Δp is the applied trans-membrane pressure. P_w^H was taken as the average of the results obtained at 50, 60, 70 psi. Diffusive water permeability was then calculated as follows [33–35],

$$P_w^D = P_w^H \frac{RT}{\bar{V}_w}\left[\frac{1-K_w}{\delta}\right] \quad (9)$$

where R is the gas constant, T is the absolute temperature and δ is the thermal non-ideality. In this work, the value of δ was set to unity following the approach adopted in our previous work on triptycene-based polysulfone copolymers [18], where comparisons between the simplified calculations and the Flory-Huggins theory model revealed qualitatively similar results. Therefore Eq. 9 can be simplified as:

$$P_w^D = P_w^H \frac{RT}{\bar{V}_w}(1 - K_w) \quad (10)$$

The average water diffusivity, D_w, was calculated as follows [34],

$$D_w = \frac{P_w^D}{K_w} \quad (11)$$

As an alternate analysis, the method of single-point fit was used to evaluate δ as detailed in the Supplementary Information (SI).

197 *2.5. Salt transport and rejection measurements*

198 The salt permeability was measured at 25 °C using a dual chamber permeation cell, which
199 consisted of two well-stirred reservoirs with a film clamped in between. The PENT-BP(H)
200 membranes were stored in 1 M NaCl aqueous solution prior to tests. One reservoir was initially
201 filled with 20 mL 1 M NaCl aqueous solution and the receptor contained 20 mL DI water. The
202 conductivity of receptor chamber was monitored over time using a conductivity meter (Oakton®
203 Con 11) and then converted to concentration via a calibration curve. Assuming pseudo-steady-
204 state permeation, the salt permeability, P_s, was found by plotting the obtained time-dependent
205 concentration data according to Eq. 12 [36],

206 $$\ln\left[1 - 2\frac{C_R(t)}{C_D(0)}\right]\left[-\frac{Vl}{2A_s}\right] = P_s t \quad (12)$$

207 where $C_R(t)$ is the salt concentration in the receptor chamber at time t, $C_D(0)$ is the initial donor
208 concentration (1 M), V is the chamber volume (20 mL), A_s is the effective film area (0.97 cm^2)
209 and l is the hydrated membrane thickness measured immediately after the salt permeation test.

210 The salt sorption coefficient (or, salt partition coefficient), K_s, defined as the ratio of salt
211 concentration in membrane to external salt concentration, was determined from a kinetic
212 desorption experiment following reported method [37]. The hydrated PENT-BP(H) membranes
213 were immersed in 50 mL 1 M NaCl aqueous solution for 2 days followed by desorption in DI
214 water for another 2 days [18,37]. The desorption salt concentration was measured by ion
215 chromatography (Dionex ICS-5000), and K_s was calculated as the ratio of salt extracted per unit
216 volume of hydrated film to initial external solution concentration:

217 $$K_s = \frac{C_d V_d}{C_0 V_m} \quad (12)$$

where C_d is the desorption salt concentration, V_d is the desorption solution volume (20 mL), C_0 is the initial external concentration (1 M NaCl), and V_m is the volume of hydrated membrane. Average values were obtained and reported from at least three specimens for each film. The salt diffusion coefficient, D_s, was then determined as follows,

$$D_s = \frac{P_s}{K_s} \tag{13}$$

The salt rejection, *R*, of PENT-BP 1:2-40(H) and PENT-BP 1:1-40(H) films was measured using a dead-end stainless-steel permeation cell (HP4750 stirred cell, Sterlitech Corp). The feed solution was 2000 ppm (0.034 M) NaCl aqueous solution that was well stirred (300 rpm) during tests [16]. For each PENT-BP membrane, three samples of ~0.5 g permeate were collected at 200, 300 and 400 psi (13.8, 20.7 and 27.6 bar) separately and the average values were reported. Feed and permeate salt concentrations were measured using ion chromatography. The salt rejection, *R*, was calculated as follows:

$$R = 1 - \frac{C_p}{C_f} \tag{14}$$

where C_p and C_f are the concentrations of permeate and feed, respectively.

3. Results and discussion

*3.1. Polym*er *properties*

The PENT-BP copolymers were prepared via condensation polymerization as shown in Scheme 1. The pentiptycene molar content (33% to 50%) and sulfonation degree (30% to 40%) were adjusted to allow systematic investigation of the structure-property relationship for these new pentiptycene-containing sulfonated polymers and elucidation of the effect of bulky

239 pentiptycene unit on water/salt transport properties. The sulfonation level was limited to below
240 50% to ensure high water/salt selectivity. The chemical structure and the composition of
241 pentiptycene-containing copolymers were confirmed by ^{1}H NMR. Figure S1 shows a
242 representative ^{1}H NMR spectrum of the PENT-BP 1:2-40(K) copolymer with peak assignments
243 and the corresponding structure. The actual molar content of pentiptycene unit in the copolymers
244 was determined from the integration ratio of characteristic peak associated with PENT or BP
245 moieties in the NMR spectra. Similarly, the sulfonation degree was determined by the peak
246 integration ratio of SDCDPS/DFDPS, which matched the target values, indicating successful
247 synthesis of pentiptycene-containing ionomers with well-controlled compositions.

248 To elucidate the effect of pentiptycene moiety on water and salt transport properties,
249 experimental results of PENT-BP membranes were compared with triptycene-containing
250 polysulfone series (TRP-BP) and non-iptycene-containing BPS(H) series that we reported earlier
251 [18]. As shown in Table 1, PENT-BP(H) membranes have lower densities than BPS(H) or TRP-
252 BP(H) series at equivalent sulfonation degree, suggesting that incorporation of bulky
253 pentiptycene units might effectively disrupt the chain packing and generate larger fractional free
254 volume, allowing for potentially higher permeability as demonstrated in our studies of
255 pentiptycene-based polymer membranes for fuel cell and gas separations [17,19]. Within the
256 pentiptycene copolymer series, the dry polymer density decreased with pentiptycene content at
257 given degree of sulfonation: at 30% sulfonation, the 1:2 PENT:BP sample had a density of 1.31
258 g/cm^3 while the 1:1 PENT-BP sample had a density of 1.24 g/cm^3 and at 40% sulfonation, the
259 1:2 PENT:BP sample had a density of 1.33 g/cm^3 versus 1.31 g/cm^3 of 1:1 PENT-BP. This
260 observation provides further evidence that the bulkiness of pentiptycene unit is effective in
261 disrupting the chain packing.

Despite of the potentially higher free volume suggested by the lower dry polymer density, the water sorption coefficients (K_w) of the acid-form PENT-BP(H) are lower than TRP-BP(H) series and BPS(H) series at similar sulfonation degree. For example, the water content of PENT-BP 1:2-40(H) is ~40% lower compared to BPS(H)-40, TRP-BP 1:1-35(H) and TRP-BP 2:1-35(H). BPS(H)-30 takes nearly 30% more water than PENT-BP 1:2-30(H) and PENT-BP 1:1-30(H). While the decreased water content of hydrated PENT-BP(H) membranes seems to contradict Yasuda's free volume theory that predicts higher water content in hydrated membrane with increased free volumes [36], there are multiple factors that regulate the water content of hydrated membranes, including ion exchange capacity (IEC), fractional free volume, and intra- and intermolecular interactions such as π-π stacking, that should be considered. For example, due to higher molecular weight of the repeat unit upon the incorporation of pentiptycene moiety, the PENT-BP(H) copolymers have lower IEC or ion concentration than BPS(H) and TRP-BP(H) series at equivalent sulfonation degree (cf. Supplementary Information). Additionally, the hydrophobicity of pentiptycene scaffolds composing 5 fused arene rings could also affect the water absorption. Measurement of water contact angles on select PENT-BP and TRP-BP series were conducted to analyze the hydrophobility of the copolymers. As show in Table S4, the PENT-BP copolymer films exhibited higher water contact angles than TRP-BP ones with similar or even lower IECs, confirming the increased hydrophobicity upon the incorporation of pentiptycene units. Despite of the additional internal free volume delineated by the benzene "blades" [22,38,39], they could also serve as molecular baffles preventing the penetration of water molecules leading to low water content.

Membranes	Dry density (g/cm^3)	K_s [a]	K_w	D_w [b] ($\times 10^{-6}$ cm^2/s)	D_s [c] ($\times 10^{-7}$ cm^2/s)	P_w^H [d] ($L \cdot \mu m/m^2 \cdot h \cdot bar$)	P_w^D [e] ($\times 10^{-6}$ cm^2/s)	P_s [f] ($\times 10^{-9}$ cm^2/s)
PENT-BP 1:2-30(H)	1.31 ± 0.04	0.075 ± 0.006	0.23 ± 0.02	6.3±0.8	0.9±0.1	0.49±0.03	1.4±0.1	6.6±0.1
PENT-BP 1:1-30(H)	1.24 ± 0.02	0.103 ± 0.030	0.21 ± 0.01	5.6±0.4	0.5±0.1	0.39±0.02	1.2±0.1	5.0±0.2
PENT-BP 1:2-40(H)	1.33 ± 0.01	0.143 ± 0.011	0.29 ± 0.02	24.4±2.4	6.4±0.6	2.61±0.06	7.1±0.3	92±6
PENT-BP 1:1-40(H)	1.31 ± 0.01	0.171 ± 0.028	0.27 ± 0.01	11.5±0.7	1.6±0.3	1.10±0.03	3.1±0.1	27.5±2.1
TRP-BP 1:1-35(H) [18]	1.41 ± 0.04	0.105 ± 0.005	0.46 ± 0.01	12.6 ± 0.9	6.9 ± 0.9	2.8 ± 0.2	5.8 ± 0.4	74 ± 1
TRP-BP 1:1-35 [g] [18]	1.43 ± 0.03	0.050 ± 0.008	0.38 ± 0.01	3.4 ± 0.4	1.2 ± 0.2	0.55 ± 0.07	1.3 ± 0.2	5.8 ± 0.1
TRP-BP 2:1-35(H) [18]	1.37 ± 0.06	0.094 ± 0.003	0.48 ± 0.01	12.0 ± 0.4	8.2 ± 0.3	2.9 ± 0.1	5.8 ± 0.2	76 ± 2
TRP-BP 2:1-35 [g] [18]	1.39 ± 0.06	0.066 ± 0.004	0.36 ±0.01	5.1 ± 0.5	1.5 ± 0.2	0.75 ± 0.07	1.8 ± 0.2	9.2 ± 0.9
BPS-30 [g][16]	1.353[40]	0.030	0.19	3.6	0.38	0.22	0.68	1.5
BPS-40 [g][16]	1.358[40]	0.043	0.29	6.1	3	0.65	1.8	8.7
BPS(H)-30 [16]	1.370[40]	0.036	0.32	12	5.5	0.89	2.3	22
BPS(H)-40 [16]	1.420[40]	0.081	0.48	18	20	4.4	8.7	226

Table 1. Density and Transport Properties of PENT-BP Polymers at 25 ºC.

[a] Measured via kinetic desorption experiment at 25 ºC (initial concentration of NaCl solution = 1M).
[b] Calculated from water sorption coefficient and diffusive water permeability using Eq. 11.
[c] Calculated from salt sorption coefficient and salt permeability according to Eq. 13.
[d] Measured at 25 ºC using dead-end filtration (feed pressure = 50, 60, 70 psi).
[e] Calculated using water sorption coefficient and hydraulic water permeability by Eq. 10.
[f] Measured at 25 ºC using direct permeation cell (donor concentration = 1 M NaCl and receptor filled with DI water initially)
[g] Salt-form (K^+) membranes of corresponding polymers without boiling in acid.

292 *3.2. Water transport*

293 Our previous study reported that incorporating triptycene into sulfonated polysulfone
294 backbone structure could increase hydraulic water permeability due to more water sorption
295 enabled by higher free volume introduced by triptycene units relative to non-triptycene-
296 containing polysulfone series [18]. It is noted that incorporation of pentiptycene units, however,
297 reduced hydraulic water permeability as compared to BPS(H) series at equivalent sulfonation
298 degree (Table 1), which could be ascribed to the lower IEC and water content in pentiptycene-
299 containing series. The free-volume theory of Yasuda et al. [36] suggested that water diffusion
300 coefficient D_w varies exponentially to volume fraction of water by assuming a linear relation
301 between free volume and volume fraction of water, i.e., log (D_w) scales linearly with $1/K_w$. To
302 further analyze the water transport, effective water diffusivity, D_w, of BPS(H), TRP-BP(H) and
303 PENT-BP(H) series are plotted versus $1/K_w$ in Fig. 1(a). In general, the water diffusion
304 coefficients of sulfonated polysulfones follow the trend predicted by Yasuda's theory [36].
305 Within the PENT-BP(H) series, increasing pentiptycene content and decreasing sulfonation
306 degree seemed to reduce the diffusive water permeability due to their reduced IEC and water
307 sorption. In contrast to the unusual suppression effect on water diffusion observed in TRP-BP(H)
308 series, the PENT-BP(H) series exhibited greater diffusion coefficients compared to BPS(H)
309 membranes at comparable water content. For example, PENT-BP 1:2-40(H) has a higher D_w
310 value than BPS-40 and BPS(H) 30 (Table 1). This phenomenon might result from the interplay
311 between multiple factors. Although the benzene blades could serve as molecular baffles and
312 make the pathways tortuous [18], the incorporation of bulky, space-occupying pentiptycene unit
313 could also generate additional free volume for small molecule transport. The diffusive water
314 permeability, P_w^D, defined by Eq.10 is plotted again $1/K_w$ as shown in Fig. 1(b). The PENT-BP(H)

series show lower diffusive water permeability than BPS(H) membrane at equivalent sulfonation degree due to relatively lower IEC. However, at comparable water content, PENT-BP 1:2-40(H) and PENT-BP 1:1-40(H) exhibit higher water permeability values than BPS(H)-30 and BPS(H)-40 (Table 1). Compared with TRP-BP(H) series, the PENT-BP(H) series displayed higher or comparable diffusive water permeability with much lower water content, which could be ascribed to the configuration of pentiptycene unit. Pentiptycene, composed of 5 arene rings, have more open clefts or "internal free volume" than triptycene and the size of microcavities is comparable with the kinetic diameters of water molecule [39]. Even with lower water content due to the hydrophobicity of arene blades, the larger cavity promotes the water transport across the membranes.

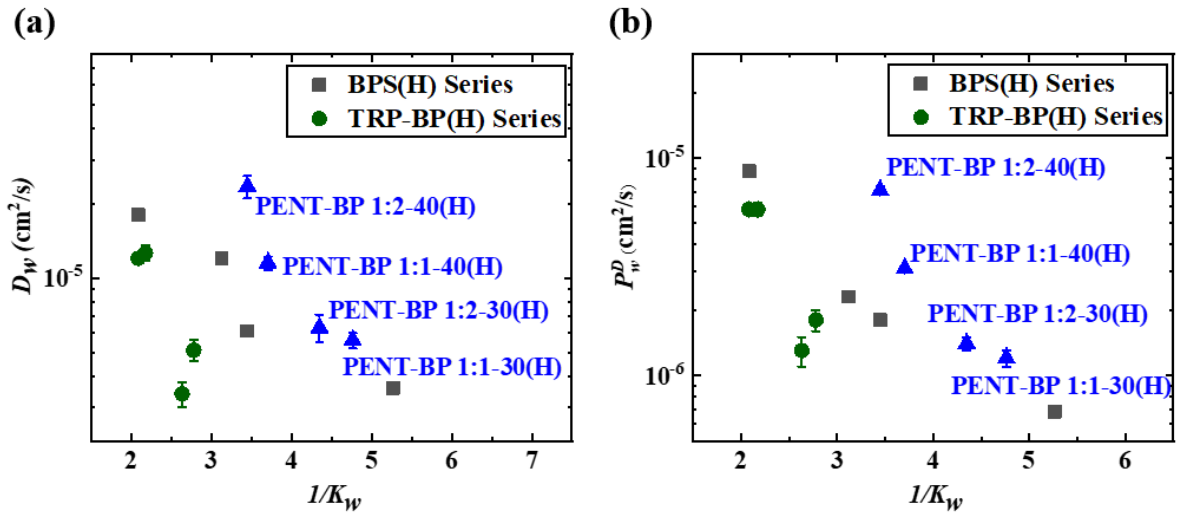

Fig. 1. (a) Water diffusivity, D_w, as a function of $1/K_w$; (b) Diffusive water permeability P_w^D as a function of $1/K_w$. D_w was calculated from P_w^D and K_w by Eq. 11. P_w^D values were calculated from hydraulic water permeability and water sorption coefficient from Eq. 10.

329 *3.3. Salt transport*

330 The salt sorption coefficients, K_s, were determined from the desorption method as described
331 in the experimental section, and the results are presented in Fig. 2. In general, K_s is positively
332 related with K_w, i.e., materials with higher water content tend to absorb more salt [29]. Since it is
333 normally assumed that pure polymers are not able to dissolve any salt [36], the distribution of
334 absorbed water and the polymer/ion/water interactions may significantly affect the salt partition
335 coefficient [41]. As shown in Fig. 2, the salt sorption coefficients of PENT-BP(H) series are
336 obviously higher than those of TRP-BP(H) and BPS(H) materials even when they share similar
337 water content. Additionally, while the water content decreased with increasing the pentiptycene
338 content due to reduced IEC, PENT-BP(H) copolymers with higher pentiptycene content
339 absorbed more salt given the same degree of sulfonation. For example, PENT-BP 1:1-30(H)
340 showed lower water content but higher salt sorption coefficient compared to PENT-BP 1:2-
341 30(H). These observations seem to suggest that incorporating bulky pentiptycene units into
342 polymer backbone might introduce a different mechanism for water and salt transport from that
343 in BPS(H) and TRP-BP(H) series. The increased salt sorption might be attributed to the internal
344 microcavities delineated by pentiptycene "blades". Although the three classes of materials have
345 the same sulfonate groups and "similar" polymer backbones, the cavities generated from the
346 pentiptycene blades might be able to accommodate more salt molecules.

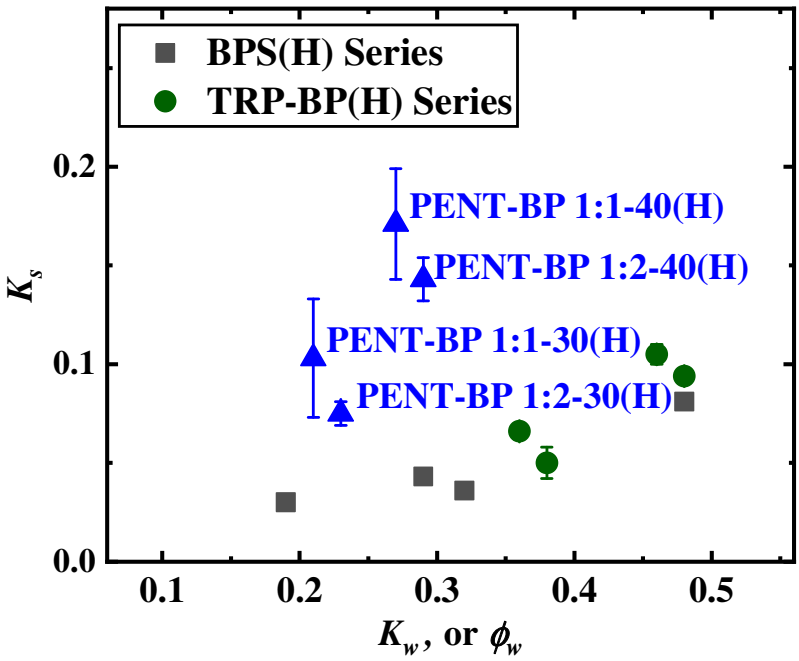

347

348 **Fig. 2.** Salt sorption coefficient (K_s) as a function of water sorption coefficient, K_w.

349 Fig. 3(a) presents salt permeability as a function of $1/K_w$. The NaCl permeability coefficients
350 were determined from direct permeation experiments using a 1 M NaCl feed concentration
351 following previous studies [16,18]. According to Yasuda's study [36], the salt permeability in
352 uncharged hydrogels is expected to scale exponentially with $1/K_w$ in a wide range as depicted as
353 a solid line in Fig. 3(a). It seems that the salt permeability in PENT-BP(H) series exhibited
354 similar trend. Compared to TRP-BP(H) and BPS(H) series, the salt permeability values of
355 PENT-BP(H) copolymers are higher at comparable water content. This observation is consistent
356 with the higher diffusive water permeability of PENT-BP(H) series as discussed in section 3.2.
357 This is a reasonable trend since salt could only permeate through water assuming that the
358 polymer matrix doesn't dissolve salt. By adjusting the sulfonation degree and pentiptycene
359 content, the PENT-BP(H) copolymer series showed a wide range of salt permeability depending

360 on the water content, suggesting excellent tunability in membrane separation performance
361 enabled by the incorporation of pentiptycene into sulfonated polysulfones.

362 Fig. 3(b) presents the salt diffusivity, D_S, determined from salt sorption coefficients and
363 permeability data, as a function of $1/K_w$. Based on the free volume theory, the salt diffusion
364 coefficient is expected to scale exponentially with free volume (volume fraction of diluent). By
365 assuming that salt doesn't permeate through polymer matrix alone, Yasuda proposed the
366 following correlation between D_s and K_w [36]:

367 $$\ln D_S = \ln D_0 - A(\frac{1}{K_w} - 1) \quad (15)$$

368 where D_0 is the NaCl salt diffusion coefficient in aqueous solution (1.47×10^{-5} cm^2/s) at room
369 temperature, A is a constant related to characteristic volume required to accommodate the
370 diffusing permeant molecules in the material. The NaCl diffusivity data obtained in this study
371 were plotted along with the data from Yasuda's study. To a first approximation, the data in Fig.
372 3(b) followed Yasuda's model and confirmed the positive relationship between water content
373 and salt diffusivity. The increase in salt diffusivity of PENT-BP(H) materials, compared to TRP-
374 BP(H) series, is related to the higher water permeability at comparable water content, resulting
375 from the additional free volume generated by the pentiptycene "blades". Similar to other
376 sulfonated polysulfone materials, the salt diffusion coefficients (Fig. 3(b)) show stronger
377 dependence on water content than water diffusion coefficients (Fig. 1(b)), given the larger size of
378 hydrated ions compared to the size of water molecules. For instance, D_w of PENT-BP 1:2-40(H)
379 is 4 times that of PENT-BP 1:1-30(H), while the D_s of the former is higher by a factor of 13
380 (Table 1). This phenomenon is consistent with the free-volume theory in that the diffusivity of

larger penetrants is more sensitive to changes in free volume compared to smaller penetrants [36,42,43].

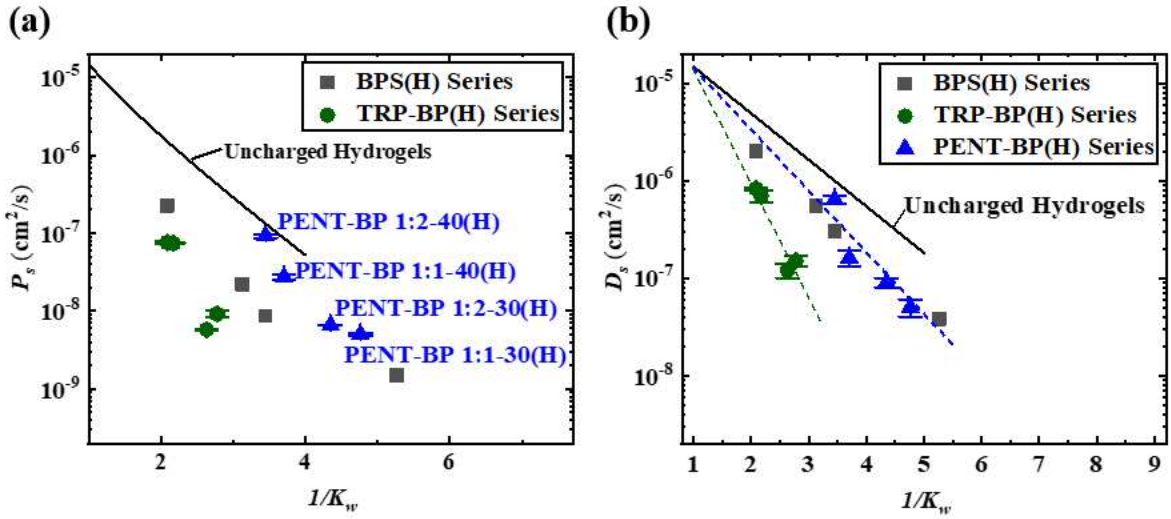

Fig. 3. (a) NaCl permeability, P_s, as a function of $1/K_w$. (b) NaCl diffusivity, D_s, as a function of $1/K_w$. P_s values were measured from direct permeation cell (initial upstream concentration = 1 M NaCl). D_s were calculated from Eq. 13. The data are compared with uncharged hydrogels (solid line) reported by Yasuda et al.[36]. The dashed lines represent the correlation between D_s and K_w from Eq. 15.

3.4. Water/salt selectivity

The separation performance of desalination membrane is often evaluated by water flux and salt rejection. High water flux with high salt rejection is pursued for the desalination applications [44–46]. However, direct salt rejection measurements are not ideal to accurately evaluate inherent separation properties of polymer materials since such measurements are very sensitive to operating factors such as salt feed concentration, membrane thickness, and applied pressures [29,40,44]. On the other hand, permeability and selectivity measurements show much less dependence on operating conditions. Therefore, the permeability data of salt and water were used

397 to determine the ideal water/salt selectivity of a polymeric film by taking the ratio of the two.
398 According to a previous study [18], diffusive water permeability, P_w^D, was calculated from Eq. 10
399 by setting the thermodynamic term δ equal to unity, and salt permeability, P_s, was calculated by
400 use of Eq. 12. Then the ideal water/salt selectivity, $\alpha_{w/s}$, is defined as the ratio of the two:

401 $$\alpha_{w/s} = \frac{P_w^D}{P_s} \quad (16)$$

402 The correlation between the water/salt selectivity $\alpha_{w/s}$ and the diffusive water permeability
403 P_w^D of three acid-form materials is presented in Fig. 4. Similar to the tradeoff relations
404 observed in polymeric gas separation membranes, there was also an empirical
405 permeability/selectivity tradeoff for desalination membranes [44]. Generally, PENT-BP(H)
406 series showed simultaneous improvement in water permeability and water/salt selectivity
407 compared to TRP-BP(H) and BPS(H) series, approaching the empirical upper bound. This
408 trend is more significant at higher sulfonation degree as shown in Fig. 4. For example, PENT-
409 BP 1:2-40(H) has 20% higher water permeability and comparable water/salt sieving
410 performance compared to TRP-BP 1:1-35(H), and is 70% more salt selective and ~50% more
411 water permeable than BPS(H)-35. The increase in water permeability of PENT-BP 1:2-40(H)
412 compared with TRP-BP series could be ascribed to the synergistic effect of higher IEC and
413 higher intrinsic free volume: even with lower water content in PENT-BP films, the higher
414 volume-based IEC in hydrated state of PENT-BP 1:2-40 (H) (cf. [17]) might facilitate the
415 water transport, while larger size of microcavities also might lead to increased water
416 permeability as discussed in section 3.2. Despite the obvious enhancement in water
417 permeability of PENT-BP 1:2-40 (H), the increase in salt permeability is relatively suppressed
418 (Table 1), which might be mainly ascribed to the salt sorption effect and the more porous

419 pentiptycene scaffold. The aromatic blades of pentiptycene units may serve as molecular
420 baffles and help narrow the free-volume-element size distribution [19,24,38,47] to form more
421 selective and tortuous pathways [18], enabling higher water/salt permeability selectivity.

422 Salt rejection (*R*) measurements were conducted using dead-end cell filtration method
423 (experiment details in the Supplementary Information) on PENT-BP 1:2-40(H) and PENT-BP
424 1:1-40(H) and the results are included in Fig. S5. Generally, membranes exhibit higher
425 rejection performance as feed pressure increases since water flux changes proportionally with
426 applied pressure difference across the membrane while the salt transport is relatively
427 independent of pressure. Consistent with the water/salt selectivity results, PENT-BP(H) series
428 showed higher salt rejection than BPS(H) series. For example, PENT-BP 1:2-40(H) displayed
429 prominent salt rejection performance with R=93% compared to BPS(H)-35 with salt rejection
430 of 86%. Considering their higher water permeability and water/salt selectivity, the PENT-
431 BP(H) series hold much greater potential for high-performance desalination application
432 compared to TRP-BP(H) and BPS(H) series.

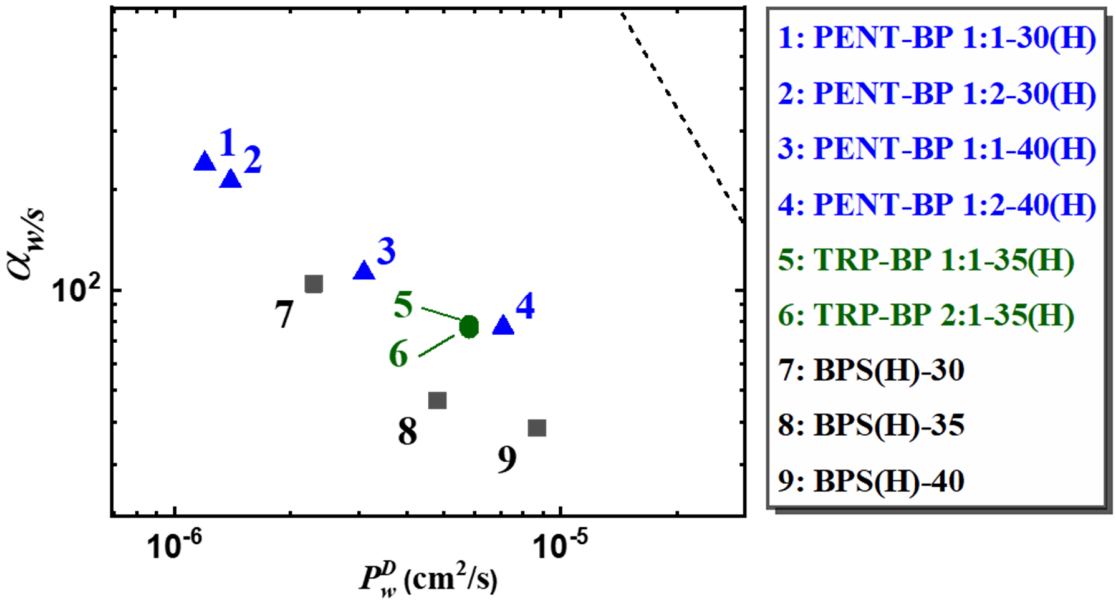

Fig. 4. The water/salt selectivity, $\alpha_{w/s}$, as a function of diffusive water permeability, P_w^D, calculated from Eq. 10 for PENT-BP(H) series (blue triangle). The data for BPS(H) series (black squares) [16] and TRP-BP(H) series (green circles) [18] are included for comparison. The solid line is the empirical upper bound [44].

Since both sorption and diffusivity contribute to the permeability, the water/salt selectivity can be further expressed in terms of water/salt sorption selectivity, $\frac{K_w}{K_s}$, and water/salt diffusivity selectivity, $\frac{D_w}{D_s}$, as follows:

$$\alpha_{w/s} = \frac{P_w^D}{P_s} = \frac{K_w}{K_s} \cdot \frac{D_w}{D_s} \quad (17)$$

Fig. 5 (a) shows the water/salt sorption selectivity as a function of water diffusivity for PENT-BP(H), TRP-BP(H) and BPS(H) series. Typically, polymers absorbing more water tend to absorb more salt leading to lower water/salt sorption selectivity, as depicted by the empirical upper bound [44]. The PENT-BP(H) series exhibits this trend of lower selectivity as higher water

sorption values, however, at noticeably lower sorption selectivity values than other sulfonated polysulfones. At comparable water content, BPS(H)-30 exhibits a water/salt sorption selectivity values 2~4 times larger than that of PENT-BP 1:2-40(H) and PENT-BP 1:1-40(H) copolymers. The reduction in water/salt sorption selectivity of PENT-BP(H) could be attributed to multiple factors. The hydrophobicity of the pentiptycene scaffolds resulted in the decreased K_w in the polymer. Meanwhile, with more sulfonated groups (higher IEC) on the polymer backbones at comparable water content, additional counterion condensation could occur in the PENT-BP 1:2-40(H) (1.35 meq/g) and the PENT-BP 1:1-40(H) (1.27 meq/g) compared to the BPS(H)-30 (1.25 meq/g), which would contribute to higher salt sorption coefficients [18,46] and lower sorption selectivity. Within the PENT-BP(H) series, at equivalent sulfonation degrees of 30% or 40%, increased pentiptycene content decreases water content/sorption coefficient but accommodated more salt molecules as discussed in section 3.2 and 3.3, resulting in lower K_w/K_s values.

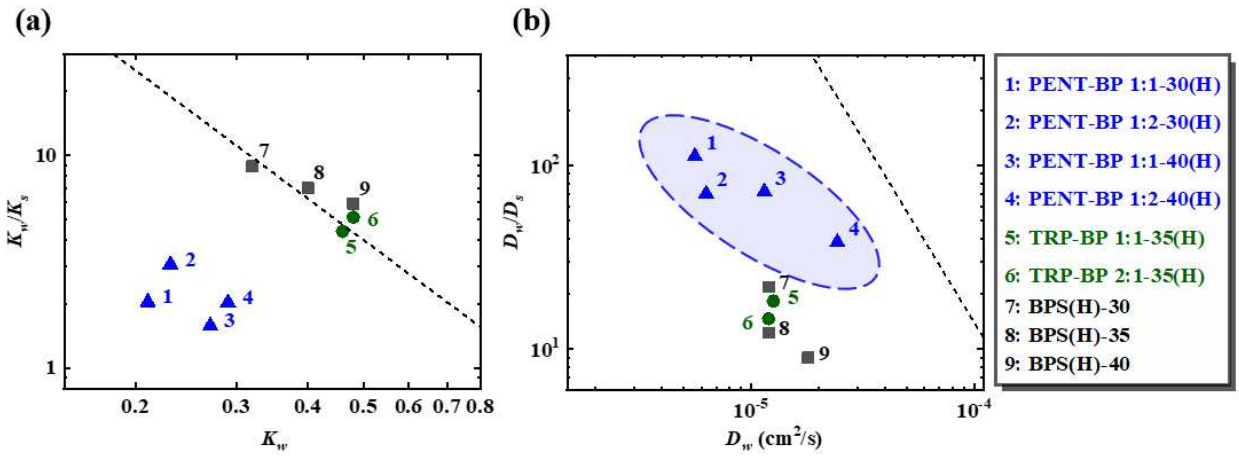

Fig. 5. (a) Sorption selectivity, K_w/K_s, as a function of K_w. (b) Diffusivity selectivity, D_w/D_s, as a function of D_w for PENT-BP(H) series (blue triangle). The data for BPS(H) series (black squares) [16] and TRP-BP(H) series (green circles) [18] are included for comparison. The dashed lines are the empirical upper bounds [44].

The data of water/salt diffusivity selectivity, D_w/D_s, as a function of water sorption coefficient are presented in Fig. 5 (b). Obviously all three series of sulfonated polysulfones show a tradeoff wherein membranes with higher water diffusivity have weaker ability to selectively sieve water from salt. However, compared to BPS(H) and TRP-BP(H) series, PENT-BP(H) series display noticeably higher D_w/D_s values in a wide range of D_w. For instance, PENT-BP 1:1-40(H) has 3-5 times greater diffusion selectivity than BPS(H)-35, TRP-BP 1:1-35(H) and TRP-BP 1:2-35(H) at comparable water diffusivity. As our previous research reported [24,39,47], the incorporation of pentiptycene in polymer backbones could generate larger fractional free volume and control the size distribution of the materials, providing an effectively tool for gas separation materials. Similar with the transport mechanisms of gas molecules, the observation here further supports that pentiptycene moieties are instrumental in fine tuning the free volume distribution and enhancing diffusivity selectivity without compromising water diffusivity. Within the pentiptycene series, incorporating more pentiptycene units or lowering sulfonation degree reduced the water diffusivity and increased the water/salt diffusivity selectivity, possibly due to increased hydropobicity. The comparison between PENT-BP 1:2-30(H) and PENT-BP 1:1-40(H), where the latter has both higher pentiptycene content and sulfonation degree, seems to suggest that the effect of pentiptycene content outweighs the effect of sulfonation degree on water diffusivity and the diffusivity selectivity. This is evidenced by the observation where PENT-BP 1:1-40(H) has ~4 times higher water diffusivity than PENT-BP 1:2-30(H) while both sharing similar water/salt diffusivity selectivity. Based on above observations, the significant improvement in water/salt selectivity by incorporating pentiptycene units could be mainly ascribed to the increased diffusivity selectivity.

4. Conclusions

Sulfonated polysulfone copolymers containing bulky pentiptycene units, PENT-BP(H), were successfully synthesized and the pentiptycene content and sulfonation degree were varied systematically to investigate the effect of pentiptycene on the water and salt transport properties. Compared to non-iptycene containing sulfonated polysulfones (i.e., BPS(H) series) and triptycene-containing ones (i.e., TRP-BP(H) series), incorporating pentiptycene moieties into polysulfone backbone enhances water and salt permeabilities and salt sorption coefficient due to the high free volume associated with bulky pentiptycene scaffold. Simultaneously, introduction of pentiptycene unit led to enhanced water/salt selectivity in PENT-BP(H) series, leading to their desalination performance approaching the upper bound. The excellent water/salt sieving ability of PENT-BP(H) and TRP-BP(H) series suggests that the intrinsic molecular free volume of iptycenes enables very promising desalination performance of polymer membranes. Further research will continue to explore a wide spectrum of iptycene-based desalination membranes with specifically designed polymer backbone structures, tailored membrane morphology using block copolymers, as well as membrane post-modification strategies to maximize desalination performance.

CRediT author statement

Tao Wang: Validation, Investigation, Formal analysis, Writing Original Draft. **Feng Gao**: Investigation, Formal analysis. **Si Li**: Investigation, Formal analysis. **William A. Phillip**: Methodology, Formal Analysis, Writing - Review & Editing. **Ruilan Guo**: Conceptualization, Methodology, Formal Analysis, Writing - Review & Editing, Supervision.

Declaration of competing interest

The authors declare no financial and personal relationships with other people or organizations that could inappropriately influence (bias) their work.

Acknowledgements

Center for Environmental Science and Technology (CEST) at Notre Dame is acknowledged for the use of some equipment. The Advanced Materials for Energy-Water Systems (AMEWS) Center at Argonne National Laboratory is acknowledged for the use of a water contact angle instrument. R.G. acknowledges the support from the Division of Chemical Sciences, Biosciences, and Geosciences, Office of Basic Energy Sciences of the U.S. Department of Energy (DOE), under award no. DE-SC0019024.

References

[1] L.F. Greenlee, D.F. Lawler, B.D. Freeman, B. Marrot, P. Moulin, Reverse osmosis desalination: Water sources, technology, and today's challenges, Water Res. 43 (2009) 2317–2348. https://doi.org/10.1016/j.watres.2009.03.010.

[2] R.F. Service, Desalination Freshens Up, Science (80-.). 313 (2006) 1088–1090. https://doi.org/10.1126/science.313.5790.1088.

[3] M. Qasim, M. Badrelzaman, N.N. Darwish, N.A. Darwish, N. Hilal, Reverse osmosis

desalination: A state-of-the-art review, Desalination. 459 (2019) 59–104. https://doi.org/10.1016/j.desal.2019.02.008.

[4] Yang, Zhou, Feng, Rui, Zhang, Zhang, A Review on Reverse Osmosis and Nanofiltration Membranes for Water Purification, Polymers (Basel). 11 (2019) 1252. https://doi.org/10.3390/polym11081252.

[5] K.P. Lee, T.C. Arnot, D. Mattia, A review of reverse osmosis membrane materials for desalination—Development to date and future potential, J. Membr. Sci. 370 (2011) 1–22. https://doi.org/10.1016/j.memsci.2010.12.036.

[6] A. a. Burbano, S.S. Adham, W.R. Pearce, The state of full-scale RO/NF desalination - results from a worldwide survey, J. Am. Water Works Assoc. 99 (2007) 116–127. https://doi.org/10.1002/j.1551-8833.2007.tb07912.x.

[7] C. Fritzmann, J. Löwenberg, T. Wintgens, T. Melin, State-of-the-art of reverse osmosis desalination, 216 (2007) 1–76. https://doi.org/10.1016/j.desal.2006.12.009.

[8] K.P. Lee, T.C. Arnot, D. Mattia, A review of reverse osmosis membrane materials for desalination—Development to date and future potential, J. Membr. Sci. 370 (2011) 1–22. https://doi.org/10.1016/j.memsci.2010.12.036.

[9] R. Haddada, E. Ferjani, M.S. Roudesli, A. Deratani, Properties of cellulose acetate nanofiltration membranes. Application to brackish water desalination, Desalination. 167 (2004) 403–409. https://doi.org/10.1016/j.desal.2004.06.154.

[10] S.S. Shenvi, A.M. Isloor, A.F. Ismail, A review on RO membrane technology: Developments and challenges, Desalination. 368 (2015) 10–26.

549 https://doi.org/10.1016/j.desal.2014.12.042.

550 [11] A.E. Allegrezza, B.S. Parekh, P.L. Parise, E.J. Swiniarski, J.L. White, Chlorine resistant
551 polysulfone reverse osmosis modules, Desalination. 64 (1987) 285–304.
552 https://doi.org/10.1016/0011-9164(87)90103-2.

553 [12] R.J. Petersen, Composite reverse osmosis and nanofiltration membranes, J. Membr. Sci.
554 83 (1993) 81–150. https://doi.org/10.1016/0376-7388(93)80014-O.

555 [13] S. Avlonitis, W.T. Hanbury, T. Hodgkiess, Chlorine degradation of aromatic polyamides,
556 Desalination. 85 (1992) 321–334. https://doi.org/10.1016/0011-9164(92)80014-Z.

557 [14] H.B. Park, B.D. Freeman, Z.B. Zhang, M. Sankir, J.E. McGrath, Highly chlorine-tolerant
558 polymers for desalination, Angew. Chemie - Int. Ed. 47 (2008) 6019–6024.
559 https://doi.org/10.1002/anie.200800454.

560 [15] J.R. Cook, Fundamental Water and Ion Transport Characterization of Sulfonated
561 Polysulfone Desalination Materials, (2014).

562 [16] W. Xie, J. Cook, H.B. Park, B.D. Freeman, C.H. Lee, J.E. McGrath, Fundamental salt and
563 water transport properties in directly copolymerized disulfonated poly(arylene ether
564 sulfone) random copolymers, Polymer (Guildf). 52 (2011) 2032–2043.
565 https://doi.org/10.1016/j.polymer.2011.02.006.

566 [17] T. Wang, T. Li, J. Aboki, R. Guo, Disulfonated Poly(arylene ether sulfone) Random
567 Copolymers Containing Hierarchical Iptycene Units for Proton Exchange Membranes,
568 Front. Chem. 8 (2020) 1–12. https://doi.org/10.3389/fchem.2020.00674.

569 [18] H. Luo, J. Aboki, Y. Ji, R. Guo, G.M. Geise, Water and Salt Transport Properties of

570 Triptycene-Containing Sulfonated Polysulfone Materials for Desalination Membrane
571 Applications, ACS Appl. Mater. Interfaces. 10 (2018) 4102–4112.
572 https://doi.org/10.1021/acsami.7b17225.

573 [19] S. Luo, Q. Liu, B. Zhang, J.R. Wiegand, B.D. Freeman, R. Guo, Pentiptycene-based
574 polyimides with hierarchically controlled molecular cavity architecture for efficient
575 membrane gas separation, J. Membr. Sci. 480 (2015) 20–30.
576 https://doi.org/10.1016/j.memsci.2015.01.043.

577 [20] J. Yang, C. Ko, Pentiptycene Chemistry: New Pentiptycene Building Blocks Derived from
578 Pentiptycene Quinones, J. Org. Chem. 71 (2006) 844–847.
579 https://doi.org/10.1021/jo052158d.

580 [21] Y. Jiang, C. Chen, Recent Developments in Synthesis and Applications of Triptycene and
581 Pentiptycene Derivatives, European J. Org. Chem. 2011 (2011) 6377–6403.
582 https://doi.org/10.1002/ejoc.201100684.

583 [22] S. Luo, Q. Zhang, Y. Zhang, K.P. Weaver, W.A. Phillip, R. Guo, Facile Synthesis of a
584 Pentiptycene-Based Highly Microporous Organic Polymer for Gas Storage and Water
585 Treatment, ACS Appl. Mater. Interfaces. 10 (2018) 15174–15182.
586 https://doi.org/10.1021/acsami.8b02566.

587 [23] R. Corrado, T.J.; Huang, Z.; Huang, D.; Wamble, N.; Luo, T.; Guo, Pentiptycene-based
588 Ladder Polymers with Configurational Free Volume for High Gas Separation Performance
589 and Physical Aging Resistance, Proc. Natl. Acad. Sci. In press (2021).

590 [24] T. Corrado, R. Guo, Macromolecular design strategies toward tailoring free volume in
591 glassy polymers for high performance gas separation membranes, Mol. Syst. Des. Eng. 5

592 (2020) 22–48. https://doi.org/10.1039/C9ME00099B.

593 [25] A.P. Isfahani, M. Sadeghi, K. Wakimoto, B.B. Shrestha, R. Bagheri, E. Sivaniah, B.
594 Ghalei, Pentiptycene-Based Polyurethane with Enhanced Mechanical Properties and CO 2
595 - Plasticization Resistance for Thin Film Gas Separation Membranes, ACS Appl. Mater.
596 Interfaces. 10 (2018) 17366–17374. https://doi.org/10.1021/acsami.7b18475.

597 [26] M. Zhang, L. Zhang, Z. Xiao, Q. Zhang, R. Wang, Pentiptycene-Based Luminescent Cu
598 (II) MOF Exhibiting Selective Gas Adsorption and Unprecedentedly High-Sensitivity
599 Detection of Nitroaromatic Compounds (NACs), Nat. Publ. Gr. (2016) 1–10.
600 https://doi.org/10.1038/srep20672.

601 [27] S. Luo, K.A. Stevens, J.S. Park, J.D. Moon, Q. Liu, B.D. Freeman, R. Guo, Highly CO 2 -
602 Selective Gas Separation Membranes Based on Segmented Copolymers of Poly(Ethylene
603 oxide) Reinforced with Pentiptycene-Containing Polyimide Hard Segments, ACS Appl.
604 Mater. Interfaces. 8 (2016) 2306–2317. https://doi.org/10.1021/acsami.5b11355.

605 [28] D. PAUL, Reformulation of the solution-diffusion theory of reverse osmosis, J. Membr.
606 Sci. 241 (2004) 371–386. https://doi.org/10.1016/j.memsci.2004.05.026.

607 [29] G.M. Geise, D.R. Paul, B.D. Freeman, Fundamental water and salt transport properties of
608 polymeric materials, Prog. Polym. Sci. 39 (2014) 1–42.
609 https://doi.org/10.1016/j.progpolymsci.2013.07.001.

610 [30] J. Cao, H. Lu, C. Chen, Synthesis , structures , and properties of peripheral o -dimethoxy-
611 substituted pentiptycene quinones and their o -quinone derivatives, Tetrahedron. 65 (2009)
612 8104–8112. https://doi.org/10.1016/j.tet.2009.07.090.

613 [31] J. Yang, C.-C. Lee, S. Yau, C. Chang, C. Lee, J. Leu, Conformation and Monolayer
614 Assembly Structure of a Pentiptycene-Derived α,ω-Alkanedithiol, J. Org. Chem. 65 (2000)
615 871–877. https://doi.org/10.1021/jo991339a.

616 [32] Y.S. Kim, M.A. Hickner, L. Dong, B.S. Pivovar, J.E. McGrath, Sulfonated poly(arylene
617 ether sulfone) copolymer proton exchange membranes: Composition and morphology
618 effects on the methanol permeability, J. Membr. Sci. 243 (2004) 317–326.
619 https://doi.org/10.1016/j.memsci.2004.06.035.

620 [33] G.M. Geise, D.R. Paul, B.D. Freeman, Progress in Polymer Science Fundamental water
621 and salt transport properties of polymeric materials, Prog. Polym. Sci. 39 (2014) 1–42.
622 https://doi.org/10.1016/j.progpolymsci.2013.07.001.

623 [34] J.G. Wijmans, R.W. Baker, The solution-diffusion model: a review, J. Membr. Sci. 107
624 (1995) 1–21. https://doi.org/10.1016/0376-7388(95)00102-I.

625 [35] D.R. Paul, Relation between hydraulic permeability and diffusion in homogeneous
626 swollen membranes, J. Polym. Sci. Polym. Phys. Ed. 11 (1973) 289–296.
627 https://doi.org/10.1002/pol.1973.180110210.

628 [36] H. Yasuda, A. Peterlin, C.K. Colton, K. a. Smith, E.W. Merril, Permeability of solutes
629 through hydrogel polymer membranes Part I. Diffusion of Sodium Chloride, Makromol.
630 Chem. 118 (1969) 19–35. https://doi.org/10.1002/macp.1968.021180102.

631 [37] G.M. Geise, C.L. Willis, C.M. Doherty, A.J. Hill, T.J. Bastow, J. Ford, K.I. Winey, B.D.
632 Freeman, D.R. Paul, Characterization of Aluminum-Neutralized Sulfonated Styrenic
633 Pentablock Copolymer Films, Ind. Eng. Chem. Res. 52 (2013) 1056–1068.
634 https://doi.org/10.1021/ie202546z.

635 [38] S. Luo, J.R. Wiegand, P. Gao, C.M. Doherty, A.J. Hill, R. Guo, Molecular origins of fast
636 and selective gas transport in pentiptycene-containing polyimide membranes and their
637 physical aging behavior, J. Membr. Sci. 518 (2016) 100–109.
638 https://doi.org/10.1016/j.memsci.2016.06.034.

639 [39] S. Luo, Q. Liu, B. Zhang, J.R. Wiegand, B.D. Freeman, R. Guo, Pentiptycene-based
640 polyimides with hierarchically controlled molecular cavity architecture for efficient
641 membrane gas separation, J. Membr. Sci. 480 (2015) 20–30.
642 https://doi.org/10.1016/j.memsci.2015.01.043.

643 [40] W. Xie, H. Ju, G.M. Geise, B.D. Freeman, J.I. Mardel, A.J. Hill, J.E. McGrath, Effect of
644 Free Volume on Water and Salt Transport Properties in Directly Copolymerized
645 Disulfonated Poly(arylene ether sulfone) Random Copolymers, Macromolecules. 44 (2011)
646 4428–4438. https://doi.org/10.1021/ma102745s.

647 [41] W. Xie, J. Cook, H.B. Park, B.D. Freeman, C.H. Lee, J.E. McGrath, Fundamental salt and
648 water transport properties in directly copolymerized disulfonated poly(arylene ether
649 sulfone) random copolymers, Polymer (Guildf). 52 (2011) 2032–2043.
650 https://doi.org/10.1016/j.polymer.2011.02.006.

651 [42] B.D. Freeman, Basis of Permeability/Selectivity Tradeoff Relations in Polymeric Gas
652 Separation Membranes, Macromolecules. 32 (1999) 375–380.
653 https://doi.org/10.1021/ma9814548.

654 [43] P.J. Flory, Thermodynamics of High Polymer Solutions, J. Chem. Phys. 9 (1941) 660–660.
655 https://doi.org/10.1063/1.1750971.

656 [44] G.M. Geise, H.B. Park, A.C. Sagle, B.D. Freeman, J.E. McGrath, Water permeability and

657 water/salt selectivity tradeoff in polymers for desalination, J. Membr. Sci. 369 (2011)
658 130–138. https://doi.org/10.1016/j.memsci.2010.11.054.

659 [45] G.M. Geise, H.-S. Lee, D.J. Miller, B.D. Freeman, J.E. McGrath, D.R. Paul, Water
660 purification by membranes: The role of polymer science, J. Polym. Sci. Part B Polym.
661 Phys. 48 (2010) 1685–1718. https://doi.org/10.1002/polb.22037.

662 [46] M. Elimelech, W.A. Phillip, The Future of Seawater Desalination: Energy, Technology,
663 and the Environment, Science (80-.). 333 (2011) 712–717.
664 https://doi.org/10.1126/science.1200488.

665 [47] S. Luo, J.R. Wiegand, B. Kazanowska, C.M. Doherty, K. Konstas, A.J. Hill, R. Guo,
666 Finely Tuning the Free Volume Architecture in Iptycene-Containing Polyimides for
667 Highly Selective and Fast Hydrogen Transport, Macromolecules. 49 (2016) 3395–3405.
668 https://doi.org/10.1021/acs.macromol.6b00485.

669